Appl. Phys. B 68, 1–5 (1999)

Applied Physics B
Lasers
and Optics

Quasi-two-dimensional dark spatial solitons and generation of mixed phase dislocations

A. Dreischuh*, G.G. Paulus, F. Zacher[CE a]

MPI für Quantenoptik, Hans-Kopfermann-Str. 1, D-85748 Garching, Germany
(Fax: +49-89/329-050, E-mail: ggp@mpq.mpg.de)

Received: 26 October 1998/Revised version: 19 January 1999

Abstract. This paper presents experimental evidence that orthogonally crossed dark soliton stripes form quasi-two-dimensional spatial solitons with a soliton constant equal to that of singly charged optical vortices. Besides the pairs of oppositely charged optical vortex solitons, the snake instability of the dark formation at moderate saturation is found to lead to generation of steering mixed edge–screw phase dislocations with zero total topological charges.

PACS: 42.65; 42.65.Tg; 42.65.Sf

Mathematically, dark optical solitons are particular solutions of the $(1+1)$-dimensional nonlinear Schrödinger equation for negative nonlinearity [1]. Physically, a spatial soliton forms when the beam interacts with the medium of propagation and changes its refractive index in a manner that leads to an exact compensation for the dark beam diffraction [2]. One-dimensional dark spatial solitons (1D DSSs) in bulk nonlinear media are experimentally generated as dark stripes [3], whereas the only truly two-dimensional DSSs are observed in the form of optical vortex solitons (OVSs) [4, 5]. The experimental formation of dark spatial solitons is inevitably accompanied by self-defocusing and intensity reduction of the finite background beam. As pointed out in the literature [6] dark pulses/beams created on finite backgrounds, even long-lived, disappear as soon as the propagation distance becomes large enough. In the strict mathematical sense they are not proper solitons. In real physical systems, losses, saturation, and higher transverse dimensionality result in nonintegrable model equations. Their solitary solutions, however, possess a large number of characteristics in common with the soliton solution of the integrable $(1+1)$-dimensional nonlinear Schrödinger equation [2]. Despite certain adiabatic relaxation characteristics these solutions are widely denoted with the term 'soliton' (see, for example, [7]) and we adopt it with this weaker meaning throughout this work.

* *Permanent address:* Sofia University, Department of Quantum Electronics, 5, J. Bourchier Blvd., BG-1164 Sofia, Bulgaria (Fax: +35-92/9625-276, E-mail: aldrei@phys.uni-sofia.bg)

Orthogonally crossed 1D DSSs are found to propagate almost independently and noninteracting thus forming quasi-2D DSSs ('fundamental dark-soliton cross', [3]). Our interest was aroused by the fact that, similarly to 1D and OV solitons [4, 8], quasi-2D DSSs should obey the guiding properties required for all-optical branching and switching applications [9]. However, these nonlinear propagation schemes will prove to be of technological importance only if they are stable under propagation. It has been shown [10] that moderate saturation of the nonlinearity can effectively suppress the dark soliton's transverse instability at the expense of weakened soliton steering [11] and reshaping [12]. In the regime of strong saturation, however, another type of instability is to be expected ([13] and Fig. 2 therein).

This paper presents comparative experimental data on the soliton constants of 1D DSSs, quasi-2D DSSs, and singly-charged OVSs generated in a thermal nonlinear medium with moderate saturation. The input dark beams with their specific phase distributions ((crossed) edge or screw dislocations) are obtained by computer-generated holograms which are of binary type and have the same grating period. The soliton constant of the quasi-2D DSS was found to be equal to that of an OVS. However, the rate at which the product of the square of the quasi-2D dark beam width and the dark irradiance tends to its asymptotic value, namely the soliton constant, corresponds to that of a 1D DSS. In this sense, the term 'quasi-2D DSS' is more precise than 'dark soliton cross'. Intentional perturbation of the quasi-2D DSS was found to result in a modulational instability and generation of 1D dark beams of finite length and mixed edge–screw phase dislocation. Although the concept of wavefront dislocations was introduced by Nye and Berry almost 25 years ago [14], this observation is, to the best of our knowledge, chronologically the third one [15] and the first to clearly identify mixed phase dislocations in the optical range.

1 Experimental setup

The experimental arrangement used is shown in Fig. 1. In order to obtain the desired phase dislocation within the dark

MS ID: APB0016
29 April 1999 15:51 CET

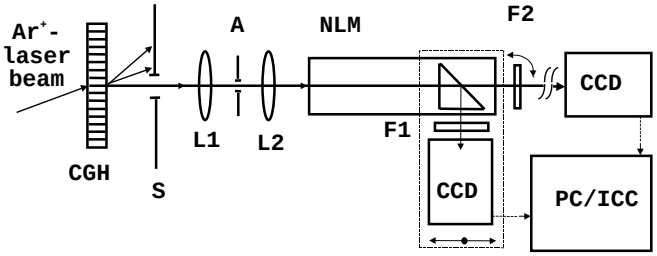

Fig. 1. Experimental setup. (CGH – computer-generated hologram; S – vertical slit; A – aperture; L1 and L2 – AR-coated lenses ($f = 80$ mm); NLM – nonlinear medium (ethylene glycol dyed with DODCI); F1, F2 – filter sets; CCD – charge-coupled-device camera with 13 μm resolution; PC/ICC – personal computer equipped with an image-capturing card)

beam, a single-line Ar^+ laser ($P_{max} = 8$ W at $\lambda = 488$ nm) is used to reconstruct the computer-generated holograms (CGHs) (Fig. 2, see also [16]). The latter were produced photolithographically on a common substrate with grating periods of 20 μm and cross sections of 5×5 mm. The diffraction efficiency in first order was measured to be 9%, this being close to the 10% limit [17] for binary holograms. The irreducible quantization noise in the reconstructed phase distribution was measured to be down to $\pi/24$ [17]. The nonlinear medium (NLM) is ethylene glycol dyed with DODCI (Lambdachrome) to reach an absorption coefficient of $\alpha = 0.107\,\mathrm{cm}^{-1}$ at $\lambda = 488$ nm. The background beam diffracted in first order with the dark formation nested in is transmitted through slit S (Fig. 1) placed some 15 cm behind the CGH and is focused on the entrance of the NLM. After covering the desired nonlinear propagation path length the dark beam is partially reflected by a prism immersed in the liquid and is projected directly on a CCD array with a resolution of 13 μm. Two filter sets (F1 and F2) are used to avoid saturation of the CCD. The immersed prism, the filter set F1, and one of the CCD cameras are mounted on a translation stage, enabling us to scan nonlinear propagation pathlengths ranging from 0.5 cm to 8.5 cm. Filter set F2 was placed on a rotation stage, allowing us to record unsaturated interference pictures after the longest NLM length of 10 cm in this experiment (with no prism immersed). The same camera is also used to monitor the far-field energy density distribution and identify the development of a modulational instability. For further evaluation the images are stored by a PC-based image-capturing card.

It should be noted that the beam directions sketched in Fig. 1 are correct with no NLM in the cell. In order to compensate for the disturbed total internal reflection at the rear face of the prism, the latter was slightly rotated. In view of the possible development of a modulational instability, great care was taken to align the optics properly and to minimize the aberrations introduced.

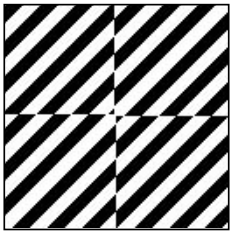

Fig. 2. Structure of the binary CGH of a quasi-2D dark beam obtained by a pure π-phase modulation of the object beam. The CGH for reconstructing 1D dark beam contains interference lines shifted along one horizontal line only

2 Comparative measurement of the soliton constants

During the measurements, the type of the incoming dark beam was changed by horizontally translating the quartz plate with the different CGHs only while keeping the alignment of the rest of the optics unchanged. In Fig. 3 we plot the product of the background beam intensity I and the square of the dark beam intensity half-width a (at 1/e level) after a nonlinear propagation path length $x = 7$ cm. The arbitrary units used are actually $(\mathrm{mW/cm^2})\mathrm{pix}^2$. The experimental points regarding the OVS formation are denoted with crosses (2D case in Fig. 3). In the evaluation of the 1D and 2D dark beam behavior the beam widths were measured vertically, whereas in the quasi-2D case the cross sections are taken at 45°. The latter results in a $2^{1/2}$ times larger quasi-2D dark beam width. The saturation behavior and stabilization of all three curves at higher powers/intensities are evident and allow comparison of the soliton constants. While the OV beam was measured to be $2^{1/2}$ times as wide as the 1D dark beam, its soliton constant was measured to be 2.2 times as large, in reasonable agreement with the expected value of 2. Within an inaccuracy of 6% the asymptotic value for the quasi-2D dark beam was found to be equal to the OVS soliton constant. However, it should be pointed out that the rate at which the quantity Ia^2 reaches the respective constant is comparable to that for the 1D DSS. In this sense we believe that the term 'quasi-2D DSS' should be used instead of 'dark soliton cross'.

Since in the presence of non-negligible absorption the nonlinear length $L_{NL} = (k_0|n_2|I_0)^{-1}$, an adequate scale of the propagation distance inside the nonlinear medium is introduced by the diffraction length $L_{Diff} = k_0 a^2(x = 0) = 1.8$ cm. The experimental data taken at nonlinear propagation path lengths x ranging from 0.5 cm to 8.5 cm (i.e. at x/L_{Diff} ranging from 0.3 to 4.8) showed conservation of the quantity $\left(Ia^2\right)|_{x=0}\,\mathrm{e}^{-\alpha x}\left\{1+(x/L_{Diff})^2\right\}^{-1}$ for all three cases consid-

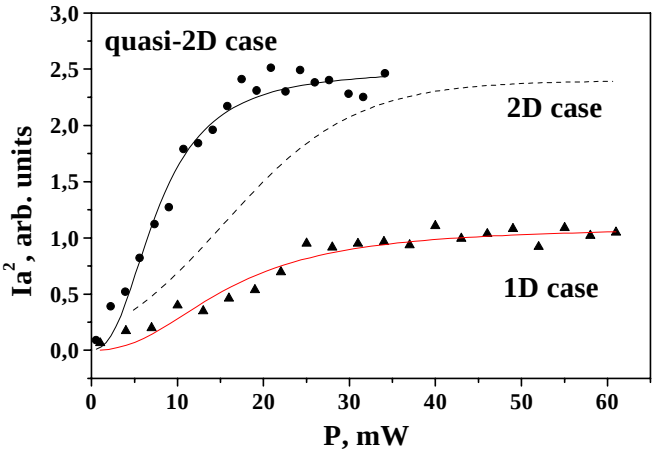

Fig. 3. Power dependence of the quantity Ia^2 measured in $(\mathrm{mW/cm^2})\mathrm{pix}^2$, which indicates the formation of 1D DSS (*lower solid curve*), OVS (*dashed curve*), and a quasi-2D DSS (*upper solid curve*). *Solid triangles* and *dots* represent the corresponding experimental data

ered. This conservation confirms the dynamic compensation of the diffraction by the nonlinearity at each particular nonlinear propagation pathlength x, at which the background beam intensity is decreased by absorption and linear (vs. intensity) defocusing. This interpretation is in agreement with the adopted content of the term 'soliton'. The measurement is performed at an input power of 50 mW and we deduced a value of $\alpha = 0.114\,\mathrm{cm}^{-1}$, this being close to the measured value of the absorption coefficient of the NLM, $\alpha = 0.107\,\mathrm{cm}^{-1}$. During the experiment pictures are recorded after all image transients had died away. The nonlinear lens itself and each unwanted beam self-bending due to a weak misalignment of the outcoupling prism are able to distort the stored image. Therefore, the last result alone should be regarded as a rather qualitative confirmation of the soliton formation.

Besides conservation of the quantity Ia^2, conservation of the total number of dark structures is one further characteristic used for identifying the formation of DSSs [2]. Continuous monitoring of the far-field power density distribution did not indicate any initiation of modulational instability followed by a decay of the dark beams. Since the thermal nonlinearity originates in the absorption and is both saturable and nonlocal, it is reasonable to expect that the stability was improved by the saturation [10].

In order to estimate the saturation intensity we conducted a self-bending experiment. No dark beam was placed on the background and the background beam itself was half-cut by a knife edge. Thereafter the transmitted half of the Ar^+ laser beam was imaged near the entrance window of the cell. The same scheme was used by Swartzlander and co-workers to study the cw self-bending effect in metal vapors [19] and in experiments on DSS formation [3]. In the absence of saturation the self-deflection should be linearly proportional to the background beam intensity (see, for example, Fig. 3 in [19]). Our data (Fig. 4) taken in the near field and after a propagation pathlength of 1.5 cm demonstrate well-pronounced saturation at powers higher than 25 mW. Since the choice of a suitable saturation model for an absorptive nonlocal nonlinearity is not trivial [20], we used a sigmoidal fit of the type $\Delta y^{SD} \approx I/(1 + I/I_{sat})^{\beta}$. The saturation power estimated was $P = 27$ mW at $\beta = 3$. Since the maximum input power in this scheme was limited to 70 mW, the maximum saturation reached was $s = I/I_{sat} = 2.6$ and can be classified as moderate [12]. The maximal nonlinear correction to the medium refractive index Δn at the largest measured saturation $s = 2.6$ was estimated to be $\Delta n = (|n_2|I_0)_{max} = 10^{-3}(\pm 15\%)$ (see also [19]).

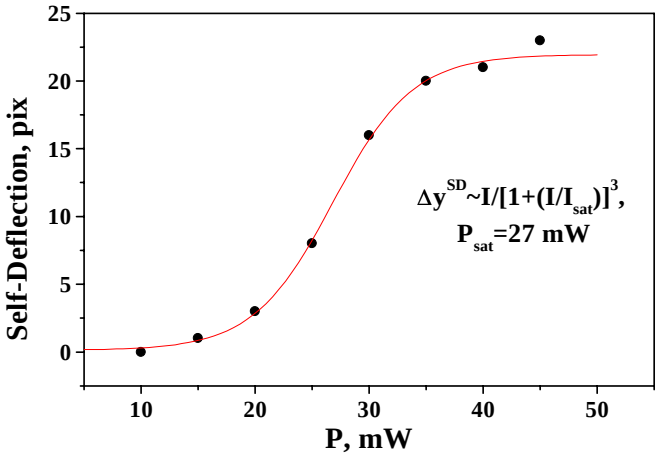

Fig. 4. Power dependence of the background beam self-deflection Δy^{SD} measured in units of camera pixels

TS[b] Figure 6 was missing in electronic form. Please check.

Editor's or typesetter's annotations (will be removed before the final TEX run)

3 Instability of the quasi-2D DSSs

The background beam radius r_{BG} is measured to be more than 20 times as wide as the OVSs and quasi-2D DSSs nested in. The modulational instability is caused intentionally by shifting the dark beams from the center of the host beam by approximately $r_{BG}/2$. All further data are recorded with no prism immersed in the NLM at a distance of 2 cm behind the exit of the cell ($x = 10$ cm).

At an input power of 70 mW (saturation $s = 2.6$) we observe snake-like bending of the 1D DSS (Fig. 5). In the final stage of the instability, pairs of interacting OVSs with opposite topological charges should appear even with saturated self-defocusing nonlinearity [20]. However, at an input power of 40 mW the decay of the quasi-2D DSS was observed to be much more spectacular.

The gray-scale image in the central part of Fig. 6 refers to a quasi-2D DSS positioned on-axis with respect to the background. The picture is recorded at $x = 8.5$ cm and

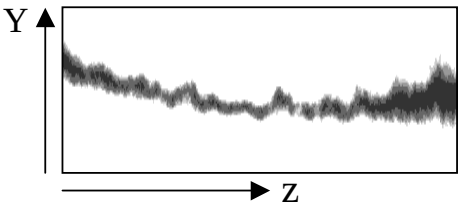

Fig. 5. Snake instability of an 1D DSS ($P = 70$ mW, $s = 2.6$, $x = 10$ cm). *Arrows* – transverse axes y and z (see also Fig. 6)

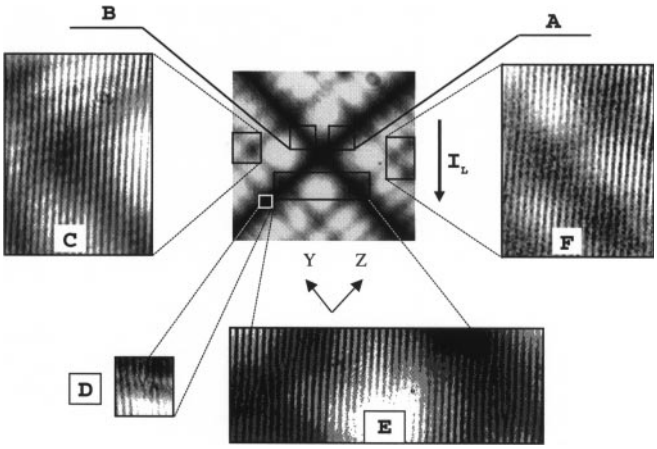

Fig. 6. Frames A to F: decay of crossed 1D dark beams under perturbation (off-axial alignment and input power of 40 mW). *Central frame*: stable dark formation obtained at on-axial alignment at 30 mW; frames D,E: pairs of OVSs; frames C,F: absence of quasi-2D gray waves; frames A,B: indications of the formation of mixed edge-screw phase dislocations (see Fig. 7 and the text for details.) One period of the interference pattern corresponds to approximately 130 μm. The *vertical arrow* indicates the increase of the local intensity TS[b]

$P = 30$ mW. It is intended to serve for a better intuitive understanding of the instability of the shifted quasi-2D dark beam in different spatial regions. The frames labeled with A–F are magnifications of the marked parts but at an input power of 40 mW, where the instability is clearly visible. A very eye-catching difference between the pictures at these intensities occurs at the center of the quasi-2D DSS (not marked in Fig. 6). At $P = 40$ mW we do not observe any dark formations there. This can be explained by the fact that the orthogonal phase dislocations encoded in the CGH (Fig. 2) do not (even roughly) form a quantized screw-phase dislocation of the types employed in [4] and [21] to generate OVSs. Since the input power of 40 mW does not strongly exceed the 30–35 mW power level needed to form a quasi-2D DSS (see Fig. 3), no pair of gray 1D DSSs with appreciable contrast should be emitted (see Fig. 9a in [9]) and no additional quasi-2D gray beams should be created. The smooth interference lines crossing the dark areas in frames C and F of Fig. 6 confirm this expectation. The snake instability of the 1D dark solitons (namely the parts of the soliton stripes located far from the crossing) results in the creation of pairs of oppositely charged OVSs. They can easily be recognized in frames D and E of Fig. 6 by the converging of two neighboring equiphase lines into one. Since the input dark formation was up-shifted with respect to the axis of the background beam, the local intensity I_L in frame D is higher than that in frame E (Fig. 6). The interaction between the OVSs in frame D is stronger and the vortices are almost collapsed.

In the areas marked A and B in Fig. 6 we observe an interference pattern of a different type (see Fig. 7a,b). Between interference lines separated by approximately 780 μm for the image of Fig. 7a and by 550 μm for that of Fig. 7b the lines become slightly curved, terminate and appear again but shifted by one half of the pattern period and oppositely curved. It is known that interference lines shifted by half a period indicate the presence of the 1D π-phase dislocation, which is required for the generation of 1D DSS [2]. The adjacent dislocations observed are well separated (by approximately 250 μm and 130 μm for the cases presented in Figs. 7a and 7b, respectively), and the smooth interference lines in between are slightly curved. This is indicative of the transition of 1D phase dislocation in a smooth (plane) phase profile, most probably by pairs of opposite-phase semi-helices with a phase step of π. In order to prove this hypothesis qualitatively, we numerically simulated 1D edge π-phase dislocation of finite length (Fig. 8a) and the resulting interference pattern. The ratio between the spatial period and the dislocation length was adjusted to correspond qualitatively to that of Fig. 7a. The similarity, consisting of interference lines shifted along an imaginary line of limited length and in curved dislocation-limiting lines, is well pronounced. Considering Fig. 6d as indicative of the highest experimental accuracy in identifying pairs of OVSs, we believe that we have observed and clearly identified the creation of mixed edge–screw phase dislocations as a consequence of a modulational instability of crossed 1D dark soliton stripes at moderate saturation.

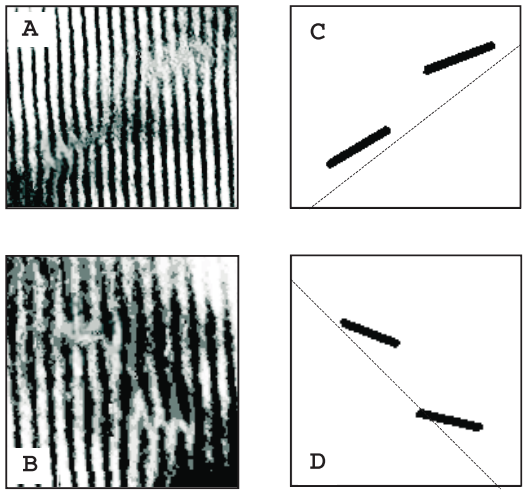

Fig. 7a–d. Experimental results (**a**,**b**) depicting the interference pattern resulting from the creation of pairs of mixed edge–screw phase dislocations in sectors A and B of Fig. 6; **c**,**d** – disposition of the dark beams formed with respect to the initial 1D dark beam axes (*dotted lines*)

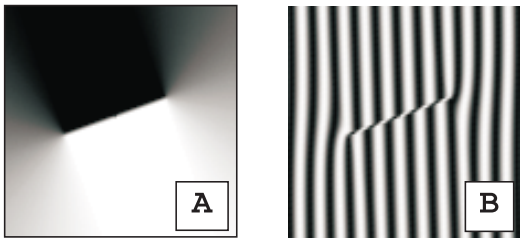

Fig. 8a,b. Phase distribution (**a**) and interference pattern (**b**) corresponding to a mixed edge–screw phase dislocation

In Figs. 7c,d we traced the 1D dark formations of finite length (bars) and their position with respect to the initial axes of the crossed 1D dark beams (dashed lines). The latter were extracted from a frame recorded at low background beam intensity. The geometrical centers of all the mixed dislocations have an offset from the axes. Since the modulational instability is initiated by an intentional offset of the dark structure from the center of the host beam, the existing gradients of the intensity could be responsible, at least partially, for the position (see, for example, Eqns. 7–9 in [22]). The dark beam steering should be expected to be influenced also by the local saturation [11]), estimated roughly to be $s = 2$. Since the mixed dislocations end with a pair of oppositely charged semi-vortices, pairs of such dislocations are likely to interact (Fig. 7a,b) and should obey their own nonlinear dynamics. Because of the phase semi-helices, to which topological charges of $\pm 1/2$ are assignable, this dynamics should not necessarily be the same as for pairs of singly- and multiply-charged OVSs [23, 24]). This is a possible explanation for the different rotation angles seen in Fig. 7c,d.

The results presented raise many new questions. Since the development of the instability obscures the further evolution stages of the dark formations, we study in a further analysis [25]) their creation and characteristics in local Kerr media under controllable initial conditions.

4 Conclusion

The results presented strongly support the statement that orthogonally-crossed dark soliton stripes form quasi-2D dark spatial solitons with a soliton constant equal to that of a fundamental OVS. The rate at which the formation asymptot-

ically reaches the soliton constant is found to be the same as that of 1D DSS, thus supporting the claim of quasi-two-dimensionality. The modulational instability was found to lead to the creation of one-dimensional dark beams of finite length and mixed edge–screw phase dislocations. In view of a further analysis carried out under controllable initial conditions [25], these beams, which to our best knowledge were observed for the first time, should be classified as steering one-dimensional odd dark beams of finite length.

Acknowledgements. A.D. would like to thank the Alexander von Humboldt Foundation for the award of a fellowship and the opportunity to work in the stimulating atmosphere of the Max-Planck-Institut für Quantenoptik (Garching, Germany). The authors are grateful to Prof. H. Walther for his continuous interest, support, and critical reading of the manuscript.

References

1. V. Zakharov, A. Shabat: Zh. Eksp. Teor. Fiz. **64**, 1627 (1973) in Russian: Sov. Phys. JETP **37**, 823 (1973)
2. G. Allan, S. Skinner, D. Andersen, A. Smirl: Opt. Lett. **16**, 156 (1991); D. Andersen, D. Hooton, G. Swartzlander Jr., A. Kaplan: Opt. Lett. **15**, 783 (1990)
3. G.A. Swartzlander Jr., D.R. Andersen, J.J. Regan, H. Yin, A.E. Kaplan: Phys. Rev. Lett. **66**, 1583 (1991)
4. G.A. Swartzlander Jr., C.T. Law: Phys. Rev. Lett. **69**, 2503 (1992)
5. C.T. Law, G.A. Swartzlander Jr.: Opt. Lett. **18**, 586 (1993)
6. Y.S. Kivshar, B. Luther-Davies: Phys. Rep. **298**, 81 (1997); Y.S. Kivshar, X. Yang: Opt. Commun. **107**, 93 (1994)
7. M. Remoissenet: *Waves called solitons* (Springer, Berlin, Heidelberg, New York 1994)
8. R. Jin, M. Liang, G. Khitrova, H. Gibbs, N. Peyghambarian: Opt. Lett. **18**, 494 (1993); W.-H. Cao, Y.-W. Zhang: Opt. Commun. **128**, 23 (1996)
9. D. Neshev, A. Dreischuh, S. Dinev, L. Windholz: J. Opt. Soc. Am. B **14**, 2869 (1997)
10. B. Luther-Davies, J. Christou, V. Tikhonenko, Y.S. Kivshar: J. Opt. Soc. Am. B **14**, 3045 (1997)
11. W. Krolikowski, X. Yang, B. Luther-Davies, J. Breslin: Opt. Commun. **105**, 219 (1994)
12. V. Tikhonenko, Y.S. Kivshar, V.V. Steblina, A.A. Zozulya: J. Opt. Soc. Am. B **15**, 79 (1998)
13. Y.S. Kivshar, W. Krolikowski: Opt. Lett. **20**, 1527 (1995)
14. J.F. Nye, M.V. Berry: Proc. R. Soc. London A **336**, 165 (1974); see also W.W. Wood, A.K. Head: ibid. 191 (1974)
15. V.Y. Bazhenov, M.S. Soskin, M.V. Vasnetsov: J. Mod. Opt. **39**, 985 (1992); I.V. Basistiy, V.Y. Bazhenov, M.S. Soskin, M.V. Vasnetsov: Opt. Commun. **103**, 422 (1993)
16. N.R. Heckenberg, R. McDuff, C.P. Smith, A.G. White: Opt. Lett. **17**, 221 (1992); Z.S. Sacks, D. Rozas, G.A. Swartzlander Jr.: J. Opt. Soc. Am. B **15**, 2226 (1998)
17. W.-H. Lee: In *Progress in Optics* XVI, ed. by E. Wolf (North-Holland, Amsterdam 1978) p. 119
18. A.A. Zozulya, D.Z. Anderson, A.V. Mamaev, M. Saffman: Phys. Rev. A **57**, 522 (1998)
19. G.A. Swartzlander Jr., H. Yin, A.E. Kaplan: Opt. Lett. **13**, 1011 (1988)
20. V. Tikhonenko, J. Christou, B. Luther-Davies, Y.S. Kivshar: Opt. Lett. **21**, 1129 (1996)
21. G.-H. Kim, J.-H. Jeon, K.-H. Ko, H.-J. Moon, J.-H. Lee, J.-S. Chang: Appl. Opt. **36**, 8614 (1997)
22. D. Rozas, C.T. Law, G.A. Swartzlander Jr.: J. Opt. Soc. Am. B **14**, 3054 (1997)
23. B. Luther-Davies, R. Powles, V. Tikhonenko: Opt. Lett. **19**, 1816 (1994)
24. D. Neshev, A. Dreischuh, M. Assa, S. Dinev: Opt. Commun. **151**, 413 (1998)
25. A. Dreischuh, G. Paulus, F. Zacher, I. Velchev: Appl. Phys. B TS[C]

TS[C] Could you provide further information, please?

Editor's or typesetter's annotations (will be removed before the final TEX run)